Volume 14
Number 37
7 October 2023
Pages 4245-4374

Polymer Chemistry

rsc.li/polymers

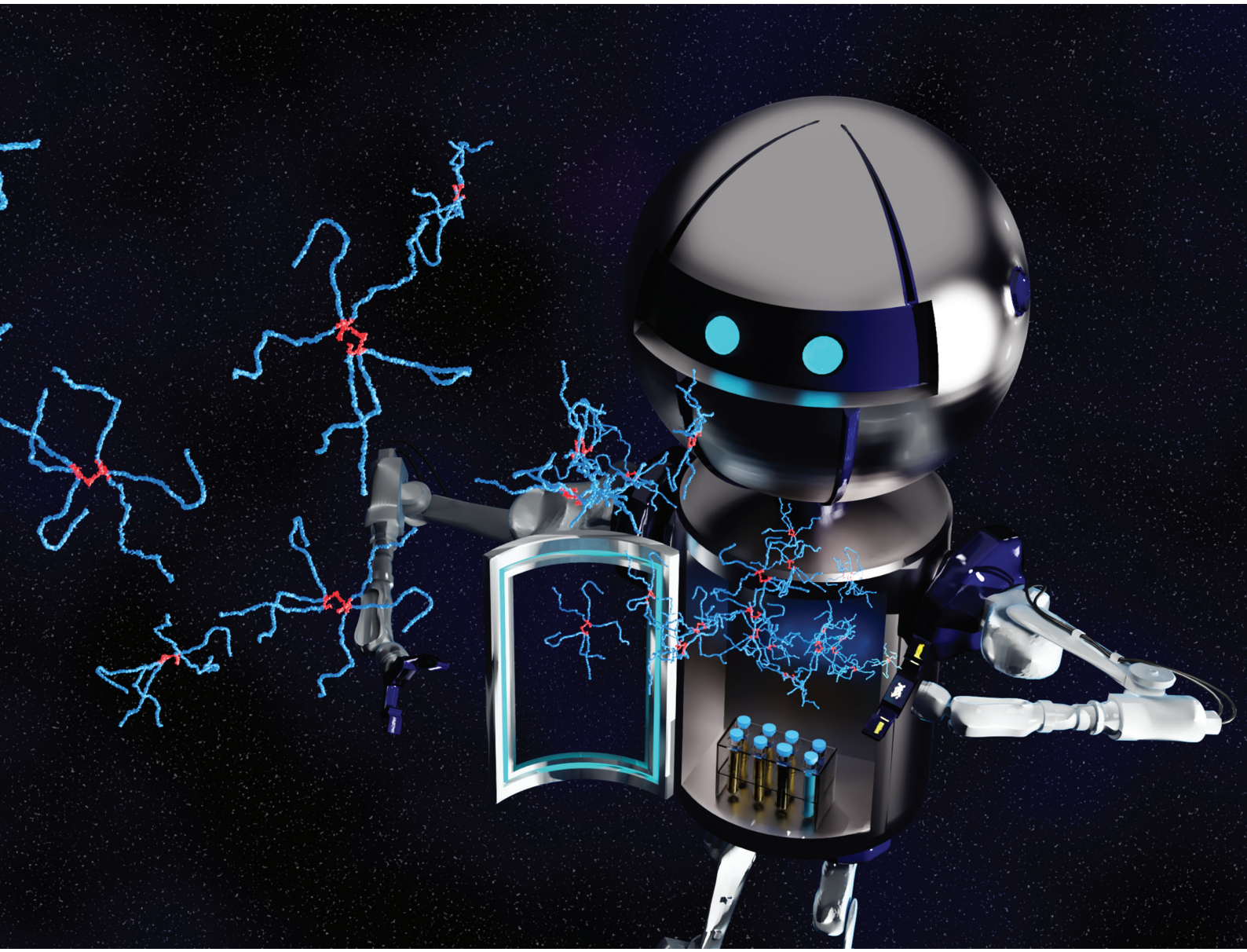

ISSN 1759-9962

ROYAL SOCIETY OF CHEMISTRY

PAPER

Daniel J. Eyckens, Ranya Simons *et al.*
High-throughput concurrent synthesis of core-crosslinked *star*-polydimethylsiloxane using an arm-first approach

Polymer Chemistry

ROYAL SOCIETY OF CHEMISTRY

PAPER

View Article Online
View Journal | View Issue

Cite this: *Polym. Chem.*, 2023, **14**, 4282

High-throughput concurrent synthesis of core-crosslinked *star*-polydimethylsiloxane using an arm-first approach†

Daniel J. Eyckens, * Shaun Howard, Graeme Moad, Benjamin W. Muir, Almar Postma and Ranya Simons *

Received 27th March 2023,
Accepted 17th August 2023

DOI: 10.1039/d3py00331k

rsc.li/polymers

In this work we use RAFT crosslinking polymerisation coupled with a Chemspeed robotic synthesis platform to optimise conditions to produce PDMS-arm star polymers by an arm-first strategy. The high-throughput polymer product library demonstrated relatively low dispersity ($Đ \approx 1.5$), high monomer conversion (>85%) and consistent size (20–40 nm). Varying the crosslinker resulted in differences in polymer product profiles as identified by size exclusion chromatography, with larger linkers between methacrylate handles causing reduced M_n and multimodal distribution compared to ethylene glycol dimethacrylate, regardless of starting arm composition or M_n. Thermogravimetric analysis revealed greater thermal stability for star polymers with increased PDMS content.

Introduction

Polymers with increased architectural complexity that offer very different properties to their linear counterparts,[1] may take a variety of forms that include stars, brushes, and gels.[2]

Recent reviews have detailed the synthesis and application of star polymers.[3–5] Three of the more common approaches are based on crosslinking polymerisation and have been categorised as the arm-first, core-first, and grafting-onto approaches.[6–8] In the arm-first method for star synthesis, a mono-end-functional linear component (the arm) is first synthesised that may be used as a transfer agent in a crosslinking polymerisation to produce a core. Most recent efforts make use of reversible deactivation radical polymerisation (RDRP),[9,10] which includes nitroxide-mediated polymerisation (NMP),[11–13] atom-transfer radical polymerisation (ATRP),[14,15] reversible addition–fragmentation chain-transfer (RAFT) polymerisation,[4,16–22] and combinations thereof.[23–25] RAFT polymerisation[26–28] has been used to produce low molar mass dispersity stars through the arm-first method.[29] These include mikto-arm stars, so-called because they comprise of arms which are compositionally diverse.[30,31] The outcome of star synthesis with respect to star molar mass dispersity, the number of arms per star, and compositional heterogeneity depends on many factors including the molar mass and composition of the arm(s) and the core, the nature of the polymerisation medium, and the concentrations of the various reaction components during polymerisation. As yet there is no consensus on the relative importance of these factors.

Siloxane-based polymers have found significant use in biological applications[32] as well as anti-fouling[33,34] and omniphobic coatings.[35,36] Their success in these applications is attributed to their unique properties, such as low surface free energy, inherent omniphobicity, and thermal stability.[37] Recent investigations demonstrate the use of RAFT polymerisation in producing siloxane containing block co-polymers, through either siloxane-based macromonomers[38] or macroRAFT (mRAFT) agents.[39–41] The preparation of siloxane-based star polymers using RAFT polymerisation has not yet been reported, though examples of star-shaped siloxanes have been obtained by other techniques such as through attachment of siloxane polymers to cyclic cores by living anionic polymerisation,[42,43] triazole-click reaction of alkyne-terminated siloxane groups to a cubic scaffold[44] or grafting of siloxane groups to a SiO_2 core.[45]

High throughput methodologies are attractive for determining optimal compositions and polymerisation conditions rapidly, and automated combinatorial approaches have previously been investigated in the optimisation of star polymer synthesis *via* NMP[46] and RAFT.[47–49] Bench-top high throughput photo-polymerisations have also been demonstrated to produce star polymers *via* RAFT polymerisation.[50] Interested readers are directed to this excellent review on high throughput polymer synthesis by Boyer *et al.*[51]

In this work, we demonstrate the use of RAFT polymerisation to produce core-crosslinked star (CCS) polymers from

Commonwealth Scientific and Industrial Research Organisation, Manufacturing, Clayton, Victoria 3168, Australia. E-mail: dan.eyckens@csiro.au, ranya.simons@csiro.au

† Electronic supplementary information (ESI) available. See DOI: https://doi.org/10.1039/d3py00331k

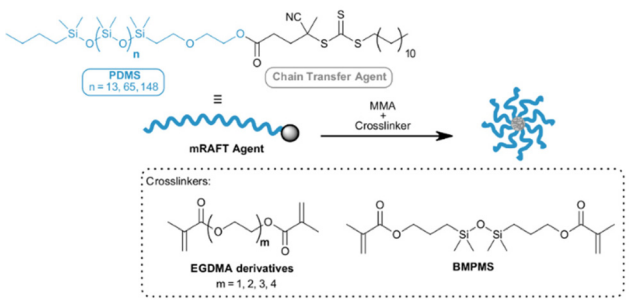

Fig. 1 Polymerisation of PDMS mRAFT agents with various crosslinkers to generate core-crosslinked stars.

polydimethylsiloxane (PDMS) mRAFT agents (Fig. 1). CCS polymers are generally accepted to have a spherical shape, with a structural density gradient from the centre of the star to the peripheral arms, often referred to as core/shell morphology.[4,52] A Chemspeed® robot[53] was utilized to execute an array of experiments in parallel, significantly reducing the need for human input in generating large sample sets. This utility determined the optimum polymerisation conditions, including ratio of crosslinker to mRAFT agent and reaction time. Previously, automated Chemspeed units have been demonstrated to optimise processes for biomass extraction,[54,55] and in the discovery of novel chemical reactions.[56] These high throughput instruments have also been applied in polymerisation reactions[57–59] including RAFT polymerisation.[60]

Experimental

Materials

The commercial RAFT agent 4-cyano-4-[(dodecylsulfanylthiocarbonyl)sulfanyl]pentanoic acid (**1**, Scheme 1) was obtained from Boron Molecular and used without further purification. Monocarbinol terminated polydimethylsiloxanes (M_n: 1000 g mol^{-1}, 5000 g mol^{-1}, 10 000 g mol^{-1}) and were obtained from Gelest and used as provided. Polyethylene glycol monomethyl ether (M_n: 2000 g mol^{-1}), 4-dimethylaminopyridine (DMAP), *N*,*N*′-dicyclohexylcarbodiimide (DCC), and 1,1′-azobis(cyclohexanecarbonitrile) (ACHN) were purchased from Sigma Aldrich and used as provided. Methyl methacrylate (MMA), ethylene glycol dimethacrylate (EGDMA), di(ethylene glycol) dimethacrylate (DiEGDMA), tri(ethylene glycol) dimethacrylate (TriEGDMA), and tetra(ethylene glycol) dimethacrylate (TetEGDMA) were purchased from Sigma Aldrich and passed through a short alumina oxide column to remove any inhibitor prior to use. 1,3-Bis(3-methacryloxypropyl)-1,1,3,3-tetramethyldisiloxane (BMPMS) was purchased from Gelest and was also passed through a short alumina column prior to use. Solvents were purchased from Sigma Aldrich and used as received unless stated otherwise.

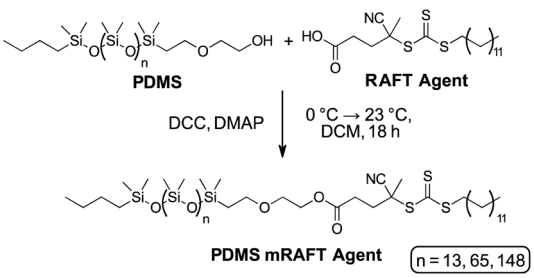

Scheme 1 Synthesis of siloxane mRAFT agents through Steglich esterification.

MacroRAFT agent synthesis

All mRAFT agents were prepared by the same general process, adapted from Duong *et al.*[39] For example: 1 kDa monocarbinol terminated polydimethylsiloxane (1.00 g, 1.00 mmol) was added to a two-neck round bottom flask under flowing N_2 gas, before dissolution in anhydrous dichloromethane (DCM, 5 mL). This solution was cooled to 0 °C, stirring, followed by the addition of dicyclohexylcarbodiimide (DCC, 1.20 mmol) and 4-dimethylaminopyridine (DMAP, 0.3 mmol). Separately, 4-cyano-4-[(dodecylsulfanylthiocarbonyl)sulfanyl]pentanoic acid (1.10 mmol) was dissolved in anhydrous DCM (5 mL). This second solution was added dropwise to the first, in 3 portions approximately 2 hours apart, maintaining the temperature at 0 °C. Following the final addition of second solution, the reaction stirred overnight (16 h), reaching ambient temperature. At the conclusion of this time, the reaction was concentrated *in vacuo*, before dissolution in *n*-heptane (20 mL) and filtering to remove dicyclohexylurea precipitate. The filtrate was then washed with MeOH (3 × 20 mL), and excess solvent removed under reduced pressure to afford a viscous yellow oil. ^{1}H NMR spectroscopy was used to show the desired compound had been produced in acceptable purity (>98%), which was confirmed by thin layer chromatography. ^{1}H NMR spectra matched literature reports.[39] ^{1}H NMR (400 MHz, $CDCl_3$): δ 4.25 (CH_2, m, 2H), 3.63 (CH_2, m, 2H), 3.43 (CH_2, m, 2H), 3.32 (CH_2, m, 2H), 2.66 (CH_2, m, 2H), 2.53 (CH_2, m, 1H), 2.42 (CH_2, m, 1H), 1.87 (CH_3, s, 3H), 1.69 (CH_2, m, 4H), 1.26 (CH_2, m, 22H), 0.88 (CH_3, m, 6H), 0.54 (CH_2, m, 4H), 0.07 (CH_3, m, 82H).

2k PEG mRAFT agent was prepared in a similar way but was isolated and purified by precipitation into *n*-heptane and subsequent filtration.

Manual RAFT experiments

All manual RAFT experiments were prepared and performed in the same manner, at the same concentration (unless otherwise stated), though may vary in scale (NMR spectroscopic experiments compared to benchtop). A specific example is given here.

1k PDMS mRAFT agent (0.094 g, 0.06 mmol, 0.015 M) was added to a round bottom flask before dissolution in toluene (4 mL). To this mixture, MMA (0.060 g, 0.6 mmol, 0.15 M), EGDMA (0.095 g, 0.48 mmol, 0.12 M) and ACHN (0.004 g, 0.018 mmol, 0.0045 M) were added whilst stirring. The reaction mixture was equipped with a rubber septum and the

mixture degassed with N_2 for at least 30 min, whilst stirring. Following this, the reaction vessel was transferred to a pre-heated oil bath (90 °C) and allowed to react for 24 h, stirring under a positive pressure of N_2. At the conclusion of this time, the reaction mixture was cooled to 0 °C to stop polymerisation and a sample was taken for NMR and SEC analysis. Excess solvent was removed under reduced pressure, and the residue taken up in the minimum amount of toluene possible. The reconstituted mixture was then precipitated into excess MeOH (repeated up to 3 times) and collected as a pale-yellow powder. Miktoarm stars could be isolated in the same way, though PEG stars required precipitation into heptane.

In the case of NMR experiments, the same method was used, though on a scale of 2 mL of toluene-d_8. A sample (0.6 mL) of this master mixture was added to a screw cap NMR tube and degassed with N_2 for 20 minutes. The sample was then added to a preheated spectrometer (90 °C) and held at that temperature for 24 h. ^{1}H NMR Spectra were collected at t = 0, 1, 2, 3, 6, 9, 12, 15, 18, 21, 24 hours.

Detail on automated RAFT experiments conducted in the Chemspeed robot can be found in the associated ESI.†

Results and discussion

Synthesis of PDMS mRAFT agents

The PDMS-based mRAFT agents were obtained under Steglich esterification conditions utilising 1k, 5k or 10k hydroxyl-terminated PDMS chains (Scheme 1).

Following work up, the desired compounds were obtained in high purity, without a need for column chromatography. Notably, to ensure high conversion the commonly used 4-cyano-4-[(dodecylsulfanylthiocarbonyl)sulfanyl]pentanoic acid chain transfer agent required addition in three parts over the course of several hours, maintaining the reaction at 0 °C. Successful coupling was evident in the ^{1}H NMR spectra (Fig. S3, ESI†) with the diagnostic chemical shift of the CH_2 adjacent to the alcohol group appearing at ~4.3 ppm compared to the starting material resonance of ~3.7 ppm.

All PDMS-based mRAFT agents were isolated in good yield and low dispersity (Table 1). For each of the compounds, the analysed molar mass (^{1}H NMR spectroscopy) was consistent with the calculated values, though some discrepancy was observed following size exclusion chromatographic (SEC) analysis. This is likely due to the different hydrodynamic volume of PDMS chains compared that of the polystyrene (PS) standards used in SEC calibration.

Table 1 Analysis of synthesised mRAFT agents

			SEC[b]		
mRAFT Agent	Yield[a]	^{1}H NMR M_n	M_n	M_w	$Đ$
1k PDMS	74%	1.6	1.4	1.5	1.08
5k PDMS	97%	5.4	4.7	4.9	1.05
10k PDMS	83%	11.5	9.1	9.4	1.03

[a] Isolated yield. [b] SEC performed in THF calibrated with PS standards. M_n values reported in kg mol^{-1}. $M_{n\ (Theoretical)}$: 1k PDMS = 1.4 kg mol^{-1}; 5k PDMS = 5.4 kg mol^{-1}; 10k PDMS = 10.4 kg mol^{-1}.

Effect of crosslinker/mRAFT agent ratio and polymerisation time

Initial benchtop experiments were undertaken to determine a preferred solvent and initiation method (Fig. S1 and discussion, ESI†). These experiments determined toluene and thermal initiation to be the preferred conditions to produce these core-crosslinked star polymers.

The use of the Chemspeed Robot allowed rapid preparation and execution of concurrent experiments to determine both the optimal ratio of crosslinker to mRAFT agent and polymerisation time. Based on a similar protocol by Ferreira *et al.*,[29] a low concentration of monomer was included to aid formation of the crosslinked core, and the amount of crosslinker was varied according to a [monomer] : [crosslinker] : [mRAFT agent] : [initiator] of $10 : X : 1 : 0.3$, where X = 2, 4, 8, or 12. For this initial investigation, the 1k PDMS mRAFT agent was used with the crosslinker ethylene glycol dimethacrylate (EGDMA) in the presence of methyl methacrylate (MMA) and ACHN. Auto-sampling of these experiments was conducted throughout the reaction at 3-hour intervals and later analysed by SEC to investigate the effect of polymerisation time (Fig. 2a).

Analysis of the progression of star formation with time revealed that 24 hours was required for maximum arm conversion and transition to a higher molecular weight polymer

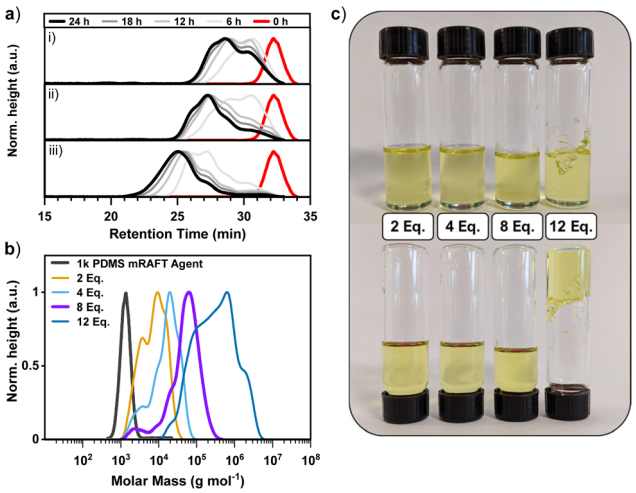

Fig. 2 (a) Size exclusion chromatograms demonstrating polymerisation progression of 1k PDMS mRAFT agent with time: [EGDMA] : [mRAFT agent] = (i) 2 : 1; (ii) 4 : 1; (iii) 8 : 1. *Note: intervals of 6 hours shown for clarity. (b) Comparison of [EGDMA] : [1k PDMS mRAFT agent] ratios after 24 hours. Bold line indicates optimal ratio of 8 : 1 ([EGDMA] : [mRAFT agent]). MWD obtained by SEC (c) Images of reaction vials following polymerisation. A ratio of 12 : 1 ([EGDMA] : [mRAFT agent]) was found to form a gel. Separated spectra are available in the ESI.† Experimental conditions: 24 hours at 90 °C in toluene. Calibrated to PS standards in THF.

(Fig. 2a). Arm conversion from initial mRAFT agent to what may be considered a 'one-armed star' is evident in the shift of the low molecular weight shoulder from the starting mRAFT agent in all examples and is due to rapid incorporation of monomer and crosslinker to the initial linear mRAFT agent.

Evidence of the optimal ratio of [EGDMA] : [mRAFT agent] = 8 : 1 is observed here and attempts at extending the reaction time beyond 24 hours in a benchtop experiment did not improve the reaction outcome (ESI†). This ratio of 8 : 1 has been reported previously in the literature for arm-first synthesis (for poly(*t*-Bu A), poly(OEG A) or poly(NIPAAm) mRAFT arms),[29] and returned the lowest dispersity of the ratios examined ($Đ$ = 1.59; entry 3, Table 2) Lower [EGDMA] : [mRAFT agent] ratios resulted in incomplete incorporation of arms and broad, multimodal distribution with lower conversion of monomers (Fig. 2a & b; entries 1 & 2, Table 2). Similarly, higher ratios of [EGDMA] : [mRAFT agent] (12 : 1) resulted in poorly resolved polymers and the formation of a gel (Fig. 2c). Analysis by SEC was complicated by the incomplete solubility of the polymer product, and though a chromatogram was obtained, it serves only as an indication of the soluble portion of the crosslinked polymer (Fig. 2b; entry 4, Table 2).

The conversion of alkene reactants was monitored by ^{1}H NMR spectroscopy to reveal the greatest incorporation of crosslinker and monomer when 10 : 8 : 1 ([MMA] : [EGDMA] : [mRAFT agent]) was employed (entry 3, Table 2). This result, coupled with the improved SEC analysis outcomes for this experiment, identified these as the optimal conditions for this system. Observation of the UV trace from SEC analysis of this sample allowed calculation of approximately 7 arms *per* star polymer for the 8 equivalents of EGDMA example (discussion and figures in ESI†).

Further investigation of this example was conducted through a ^{1}H NMR experiment, during which the sample was held at 90 °C for 24 hours and a ^{1}H NMR spectra was recorded at regular time points (Fig. 3, spectra in ESI†). Monitoring the alkene region in the ^{1}H NMR spectra revealed rapid conversion of EGDMA alkene groups, reaching 64% conversion in 3 hours, in contrast to the much slower MMA which achieved only 35% conversion in the same time span. In addition to monitoring the alkene peaks, analysis of the methylene protons of EGDMA and the methoxy group of MMA could be conducted, resulting in identical trends (Fig. S6, ESI†).

Table 2 Optimization of crosslinker/1k PDMS mRAFT agent ratio

Entry	Crosslinker Ratio	Conversion (1H NMR)[a]	M_n[b]	M_w[b]	$Đ$[b]
1	2	89%	7.4	13.0	1.76
2	4	87%	13.7	27.9	2.03
3	8	93%	46.1[c]	73.4[c]	1.59[c]
4	12	96%	95.1	368.6	3.87

[a] Total alkene conversion calculated by ^{1}H NMR spectroscopy. [b] Calculated by SEC in THF (kg mol^{-1}). [c] Data for main product peak shown.

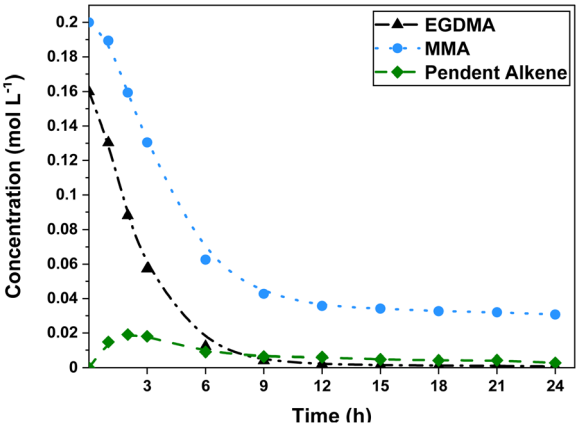

Fig. 3 Conversion of alkene protons observed by ^{1}H NMR spectroscopy. Experimental conditions: [monomer] : [crosslinker] : [mRAFT agent] : [initiator] of 10 : 8 : 1 : 0.3, 24 hours at 90 °C in toluene-d_8.

Importantly, high conversion of around 45% for the total alkene (EGDMA + MMA) component of the reaction mixture after only 3 hours is consistent with the early formation of a one-armed star observed in the SEC trace (Fig. 2a).

Evolution of pendent double bonds could be observed slightly downfield of the main alkene peaks of EGDMA and MMA (Fig. S7, ESI†) and increase in intensity to a peak value of 12% after 2 hours, followed by decline for the remaining timespan. Tripathi *et al.*[61] found the reactivity of pendent double bonds in a MMA/EGDMA copolymerisation to be around 50% of the free crosslinker species, an outcome observed here in the remaining concentration of pendent bonds compared to free EGDMA (Fig. 3).

Interestingly, MMA conversion plateaus at around 85%, though the reason for this is unclear. When considering the concentration of remaining MMA at the conclusion of the experiment (~0.030 mol L^{-1}), it roughly correlates with the difference of initial concentrations of EGDMA (0.16 mol L^{-1}) and MMA (0.2 mol L^{-1}). This suggests a close to 2 : 1 reactivity for EGDMA : MMA (due to two reactive handles), and this has be observed in the literature previously by Monte Carlo simulation (and confirmed experimentally), though not in respect to RAFT polymerisation.[61] Rosselgong *et al.* also reported similar reactivities for DSDMA and MMA in RAFT copolymerisation studies, and found that around 15% of MMA remained after 15 hours with higher conversion only achieved after 35 hours.[62] Benchtop experiments conducted in our work without the presence of MMA resulted in reduced arm incorporation (ESI†). It should be noted that manual benchtop compared to automated experiments gave near identical results regardless of scale, crosslinker, or mRAFT agent. These outcomes were reflected in SEC traces of the crude reaction mixture, and in the degree of monomer conversion (by ^{1}H NMR spectroscopy). Multiple repeats of different experiments consistently gave the same results, assuring the reliability and efficacy of using the Chemspeed robot for conducting parallel polymer synthesis.

Effect of crosslinker and arm length

With the optimal [crosslinker] : [mRAFT agent] identified as 8 : 1, the effect of arm length and crosslinker size was investigated. Arms in the form of 1k, 5k and 10k PDMS mRAFT agents were combined under the optimised conditions with crosslinkers with increasing ethylene glycol units between the methacrylate handles. The intention was to examine the influence of crosslinking density in the core and its effect on the physical characteristics of the star products. The experiments were conducted concurrently in the Chemspeed robot with either EGDMA, DiEGDMA, TriEGDMA, TetEGDMA or BMPMS as crosslinker.

Polymerisation of the 1k PDMS mRAFT agent arm with the series of crosslinkers resulted in a significant increase in molecular weight, though was not consistent across all crosslinkers (Fig. 4a). The use of EGDMA with 1k PDMS mRAFT agent produced polymers with higher molecular weight, narrow dispersity ($Đ$ = 1.59) and closer to monomodal distribution than the other crosslinkers when analysed by SEC in THF, although some evidence of the starting arm is present in the SEC trace (0.2%; calculated by integration of the main product and the mRAFT agent peaks in the crude SEC trace). The use of crosslinkers with increased distance between methacrylate groups (DiEGDMA, TriEGDMA & TetEGDMA, and BMPMS, Fig. 4a) consistently resulted in molecular weights one order of magnitude greater than that of the starting mRAFT agent, though significant shoulders to higher molecular weight is observed. These multimodal peaks indicate incomplete conversion to a uniform polymer product. It is possible that the higher molecular weight outcome (polymer products of EGDMA) may be due to star–star coupling, though formation of a defined 'single-star' polymer product was not evident for the EGDMA sample during the time points initially investigated in this study (Fig. 2a-iii). Alternatively, it is possibly that increased distance between methacrylate handles facilitates *intra*molecular crosslinking over *inter*molecular crosslinking. If this is the case, mid-range M_n values for polymer products based on DiEGDMA, TriEGDMA, TetEGDMA and BMPMS crosslinkers could be the result of fewer arms incorporated *per* polymer structure, despite good conversion of alkene groups by ^{1}H NMR spectroscopy (Table 3). These findings are consistent with literature examples of longer aliphatic crosslinkers resulting in lower M_n of star products in similar systems.[29] Indeed, work by Rosselgong *et al.* identifies lower concentrations (≤30 wt%) of MMA with disulfide dimethacrylate (DSDMA) crosslinker resulting in intramolecular cyclisation dominating the polymerisation process when synthesising branched methacrylic copolymers.[63,64]

In our work, the greatest monomer/crosslinker mass percentage across all experiments was 21 wt%, suggesting a possibility of intramolecular cyclisation, particularly as DiEGDMA exhibits a similar chain length and flexibility to DSDMA as explored in other works. Nonetheless, the concentration of alkene components was limited to reduce the potential for star–star coupling events.

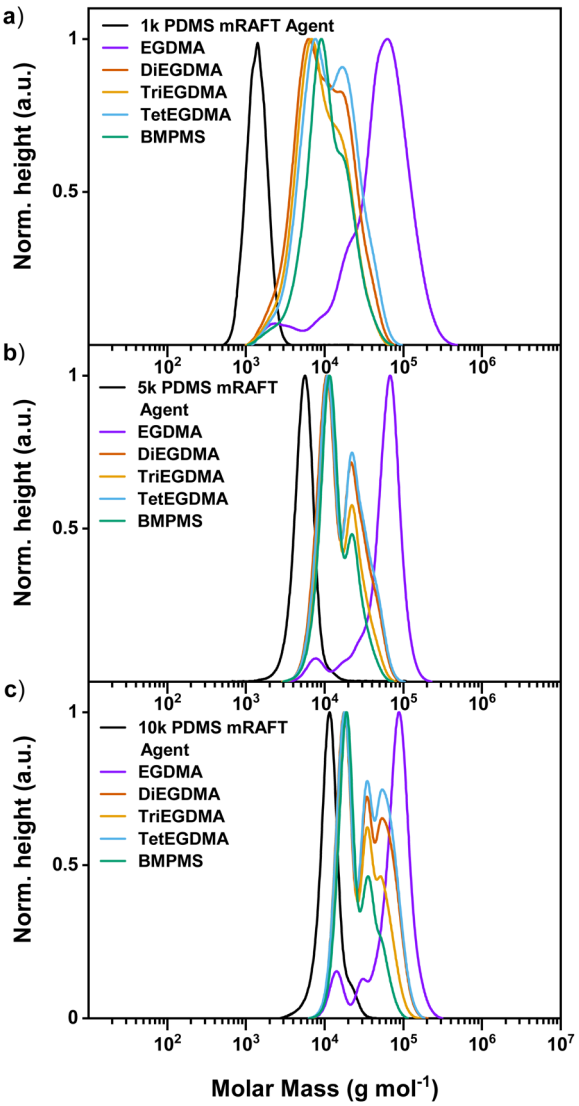

Fig. 4 MWD obtained by SEC demonstrating polymerisation of various crosslinkers with increasing mRAFT agent arm length; (a) 1k PDMS mRAFT agent; (b) 5k PDMS mRAFT agent; (c) 10k PDMS mRAFT agent. Separated spectra are available in the ESI.† Experimental conditions: [MMA] : [Crosslinker] : [mRAFT agent] : [I] = 10 : 8 : 1 : 0.3; 24 hours at 90 °C in toluene. Calibrated to PS standards in THF.

Rapid one-pot sequential aqueous RAFT (rosa-RAFT) has been employed to produce star polymers derived from arms with different monomer DP and species, in combination with different acrylate crosslinkers.[47] In that work, the largest crosslinker (PEG_{700}-diacrylate) produced core-crosslinked stars with lower molecular weight than smaller crosslinkers (diethylene glycol diacrylate) at a [crosslinker] : [mRAFT agent] ratio of 10 : 1 (using the same mRAFT agent). This suggests a similar influence of intramolecular bonding in the polymerisation process with larger distance between alkene groups. Interestingly, the use of tetra(ethylene glycol) diacrylate did not exhibit a similar outcome as the PEG_{700}-diacrylate and does not appear to suffer from intramolecular crosslinking to

Table 3 Analysis of PDMS-based star products

Entry	mRAFT agent	Crosslinker	Conversion[a] (%)	M_n[b] (kg mol^{-1})	M_w[b] (kg mol^{-1})	$Đ$[b]
1	1k PDMS	EGDMA	93	46.1[c]	73.4[c]	1.59[c,d]
2		DiEGDMA	92	7.2	12.6	1.75
3		TriEGDMA	90	7.1	11.4	1.60
4		TetEGDMA	90	8.7	14.9	1.72
5		BMPMS	90	8.6	12.9	1.50
6	5k PDMS	EGDMA	92	39.8[c]	62.2[c]	1.56[c,e]
7		DiEGDMA	91	13.7	19.6	1.42
8		TriEGDMA	89	13.1	17.3	1.32
9		TetEGDMA	88	14.3	20.4	1.43
10		BMPMS	89	12.8	16.2	1.26
11	10k PDMS	EGDMA	94	53.0[c]	81.2[c]	1.53[c,f]
12		DiEGDMA	94	26.7	39.5	1.48
13		TriEGDMA	90	24.1	32.9	1.37
14		TetEGDMA	91	27.5	40.6	1.48
15		BMPMS	91	22.2	27.7	1.25

[a] Total alkene conversion calculated by ^{1}H NMR spectroscopy. [b] Calculated by SEC. [c] Data for main product peak shown. [d] 99% arm incorporation calculated by SEC. [e] 93% arm incorporation calculated by SEC. [f] 90% arm incorporation calculated by SEC. Experimental conditions: [MMA] : [Crosslinker] : [mRAFT agent] : [I] = 10 : 8 : 1 : 0.3; 24 hours at 90 °C in toluene.

the same extent. This is likely due to these polymerisations conducted at higher concentrations than explored in our work, which improves the probability of intermolecular crosslinking, even for large, flexible crosslinkers.[63,64] It is also possible that the difference in reactivity of acrylates compared to methacrylates (used in our work) further convolutes this finding. The rapid reaction time (3 minutes) may serve to limit star–star coupling outcomes, as well as the effect of solvent, core, and arm compatibilities.

Closer examination of a longer crosslinker (TriEGDMA) with the 1k PDMS mRAFT agent was conducted *via* ^{1}H NMR spectroscopy with the presence of the pendent alkene detected and tracked throughout the 24 h experiment (ESI, Fig. S9–11†). This analysis revealed a much lower concentration of pendent alkene for TriEGDMA compared to the EGDMA example (peak concentration at 3 hours of 0.006 mol L^{-1} compared to 0.02 mol L^{-1}, respectively). This strongly supports intramolecular crosslinking being a dominating reactivity due to rapid reaction of proximal alkene species following attachment of one end of the crosslinker. Further, this example demonstrated reduced consumption of MMA compared to the EGDMA sample due to increased backbiting, resulting in stunted polymerisation to higher M_n products.

The 5k PDMS mRAFT agent demonstrated comparable results to the 1k PDMS mRAFT agent, with the highest molecular weight polymers formed with the use of EGDMA as the crosslinker (Fig. 4b). Some shouldering at lower molecular weight is observed for this example and is due to incomplete incorporation of the mRAFT agent (93% determined by SEC). Again, limited increases in molecular weight for larger crosslinkers are possibly the result of intramolecular cyclisation restricting the incorporation of a greater number of arms. Interestingly, it is more obvious in this series of polymerisations that the use of DiEGDMA or TetEGDMA trend towards higher molecular weight in the multimodal distribution than TriEGDMA or BMPMS. This suggests that an increase in distance between reactive handles leads to intramolecular crosslinking (DiEGDMA compared to EGDMA) and this effect is increased with increased chain length (TriEGDMA and BMPMS). However, further increasing the chain length (TetEGDMA) results in a flexible linker capable of intramolecular bonding, yet distal enough to also allow intermolecular bonding. This can be seen in the relative contributions of the second peak in the MWD by SEC spectra (Fig. 4b).

Indeed, this is also the case when exploring the 10k PDMS mRAFT agent in that relatively shorter crosslinkers (EGDMA) resulted in higher molecular weight star polymers (Fig. 4c), albeit with incomplete incorporation of mRAFT agent (90% determined by SEC). Again, larger crosslinkers resulted in relatively lower molecular weight increases, and the relative contributions of peak shoulders for different polymer species are comparable to the previous 5k PDMS mRAFT agent examples. Increased resolution of the contributions of different species for longer crosslinkers with increasing arm length may stem from the greater M_n contribution *per* arm compared to the 1k PDMS mRAFT agent version. The broad, multimodal distribution observed for DiEGDMA and TetEGDMA further demonstrates the different contributions of intra- and intermolecular crosslinking for these examples and may be derived from solvent compatibility effects as the siloxane content and architectural complexity increases with polymerisation.

It is interesting that EGDMA should perform so differently from the other crosslinkers explored, yet consistently across different mRAFT agents. Multimodal distribution was observed in the SEC traces for EGDMA examples in the time points leading up to 24 hours (Fig. 2), though not to the extent of the longer crosslinkers. This may be due to a critical spacer length under these conditions. It is difficult to discern exact reasoning for these outcomes, though the contribution of intra- and intermolecular crosslinking is likely a factor, as discussed. It is possible that introduction of a rigid spacer with

limited flexibility may reduce backbiting and lead to more uniform molecular weight distributions, though this is beyond the scope of the current work.

Precipitated samples of the CCS polymer examples formed from the 1k, 5k and 10k PDMS mRAFT agents with EGDMA crosslinker were investigated by NMR using diffusion ordered spectroscopy (DOSY). The 2D DOSY spectra for the mRAFT agents are shown in Fig. S12–S14† and those for the stars in Fig. S15–17.† Signals attributable to the mRAFT agent-derived arms and those attributable to the MMA/EGDMA core have the same spin diffusion time, which is consistent with them being parts of the same star molecule. Sensitivity is low, but it is nonetheless notable that there is no detectable residual mRAFT agent in the stars. As would be expected, the starting mRAFT agents display decreasing diffusion coefficients with increasing chain length and there is a linear correlation between log(M_n) and spin diffusion time for these materials (Fig. S18b†).

The peak SEC molar masses and spin diffusion time for the stars appear largely independent of the mRAFT agent molar mass (Fig. S18†).

Despite good conversion of alkene reactants across all examples, significantly lower molecular weight products and generally narrower dispersity are observed when using larger crosslinkers (Table 3). Further, the degree of increase in M_n for star products compared to initial arm M_n diminishes with increase arm length. This may be due to steric effect of forming crosslinked cores with larger arms preventing incorporation of a higher number of arms *per* structure, as well as encouraging intramolecular bonding to occur.

Given that a low monomer/crosslinker concentration (<30 wt% of solvent) has been reported to be associated with an increased propensity for intramolecular bonding,[62,65] a sample was reattempted at polymerising at both a higher concentration and for a longer time (Fig. 5).

In this example, the 5k PDMS mRAFT agent was employed with TriEGDMA at a slightly higher concentration, resulting in a multimodal distribution approaching higher molecular weight than the lower concentration example for the same time (Table S3†). Extending the reaction time for the higher concentration examples (with addition of extra initiator at 24 h) resulted in a solidified reaction mixture unable to be analysed further. Taking the original concentration and extending the reaction time to 48 h (without further addition of initiator) resulted in a dispersity somewhere in between the other two examples, with slow transition to higher M_n products, though in the same trend as the other cases. Further increasing the reaction concentration was deemed inappropriate as the mass of mRAFT agent and reactants would overcome the amount of solvent, approaching a neat reaction solution.

To examine the effect of changing the nature of the starting arm, a 2k polyethylene glycol (PEG) mRAFT agent was employed in the same conditions. Synthesis of the 2k PEG mRAFT agent was achieved in a similar method to the PDMS-mRAFT agent, in good yield (71%) and narrow dispersity ($Đ$ = 1.08; entry 1, Table 4).

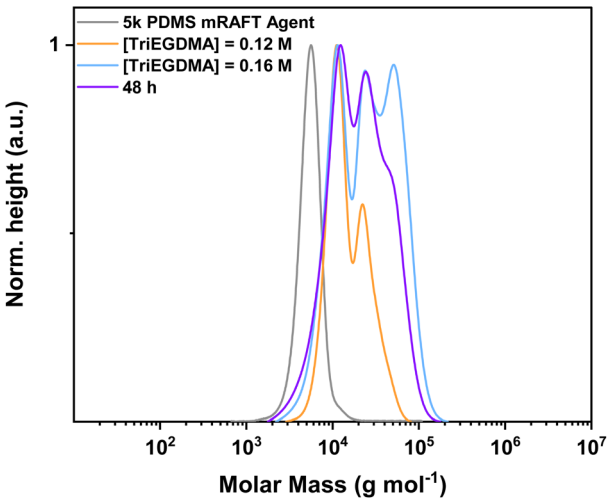

Fig. 5 MWD obtained by SEC demonstrating polymerisation of TriEGDMA with 5k PDMS-mRAFT agent at different concentrations and for different times. Separated spectra are available in the ESI.† Experimental conditions: [MMA] : [Crosslinker] : [mRAFT agent] : [I] = 10 : 8 : 1 : 0.3; 24 or 48 hours at 90 °C in toluene. Calibrated to PS standards in THF.

Employing the 2k PEG-mRAFT agent in the same conditions as the identified for the PDMS-mRAFT agents resulted in good alkene conversion (90%) and narrow dispersity ($Đ$ = 1.51) when using EGDMA as the crosslinker (entry 2, Table 4). In contrast to the high degree of arm incorporation for PDMS-mRAFT agents across all examples, the 2k PEG-mRAFT agent exhibited an arm conversion of around 88% (by SEC, Fig. 6) for the EGDMA sample, though the greatest molecular weight increase was achieved using this crosslinker. Increasing the crosslinker ratio to 12 : 1 ([EGDMA] : [mRAFT agent]) improved arm incorporation to 94% without formation of a gel and maintained a narrow dispersity for the product peak (ESI;† conversion = 95%, M_n = 67.3 kg mol^{-1}, M_w = 96.2 kg mol^{-1}, $Đ$ = 1.43).

All other crosslinkers assessed in this system demonstrated good arm incorporation, though reduced increases in molecular weight, consistent with the results of the PDMS-mRAFT agents.

Good dispersity was maintained through these examples, all of which were improved compared to the PDMS analogues. This may be due to different chemical compatibilities of the mRAFT agent with the crosslinker compared to the siloxane-based systems. Rough calculation of number of arms *per* star (Star M_n/Arm M_n) for these larger crosslinkers suggests around 5 arms in each structure and is consistent with the intramolecular crosslinking being dominant for longer crosslinkers.

Given the improved outcome observed when using EGDMA as the crosslinker, we trialled this crosslinker in generating a statistical miktoarm star based on the 5k PDMS mRAFT agent and the 2k PEG mRAFT agent used in this work (Fig. 7). Utilising equal parts of each mRAFT agent and ratios of

Table 4 Analysis of 2k PEG-mRAFT agent and PEG-based star products

Entry	mRAFT agent	Crosslinker	Conversion[a] (%)	M_n[b] (kg mol^{-1})	M_w[b] (kg mol^{-1})	$Đ$[b]
1	2k PEG	—	71[c]	2.8[d]	3.0	1.08
2		EGDMA[e]	87	62.9[e]	94.7[e]	1.51[e]
3		DiEGDMA	88	10.0	17.1	1.72
4		TriEGDMA	88	9.6	15.2	1.59
5		TetEGDMA	89	11.6	20.7	1.78
6		BMPMS	91	10.9	16.4	1.51

[a] Calculated by ^{1}H NMR for alkene component. [b] Calculated by SEC. [c] Isolated yield. [d] M_n (^{1}H NMR) = 2400 g mol^{-1}. [e] Data for main product peak shown. Experimental conditions: [MMA] : [Crosslinker] : [mRAFT agent] : [I] = 10 : 8 : 1 : 0.3; 24 hours at 90 °C in toluene.

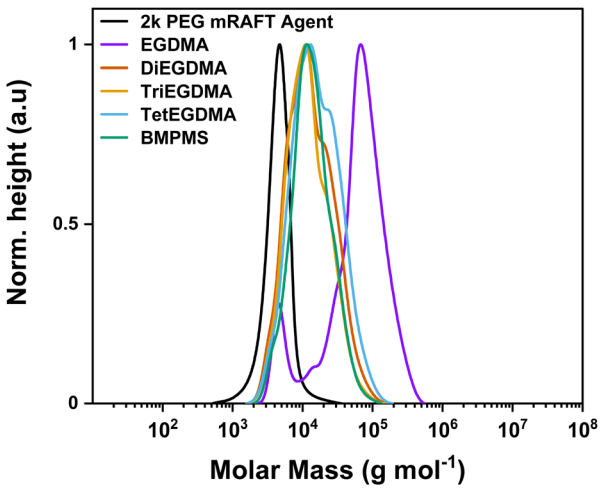

Fig. 6 MWD obtained by SEC demonstrating polymerisation of various crosslinkers with 2k PEG-mRAFT agent. Separated spectra are available in the ESI.† Experimental conditions: [MMA] : [Crosslinker] : [mRAFT agent] : [I] = 10 : 8 : 1 : 0.3; 24 hours at 90 °C in toluene. Calibrated to PS standards in THF.

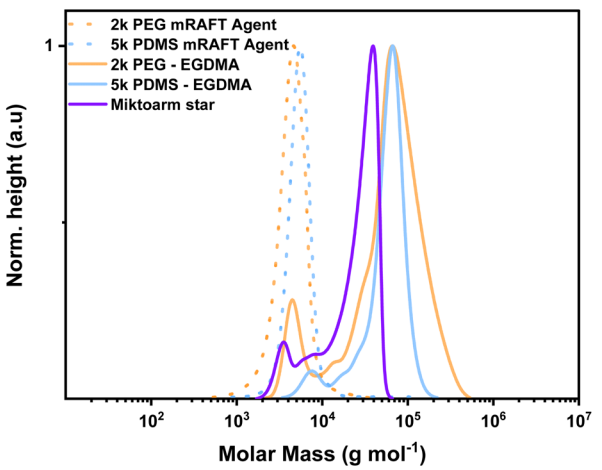

Fig. 7 MWD obtained by SEC demonstrating synthesis of a miktoarm star based on the 5k PDMS and 2k PEG mRAFT agents. Separated spectra are available in the ESI.† Experimental conditions: [MMA] : [Crosslinker] : [mRAFT agent] : [I] = 10 : 8 : 1 : 0.3; 24 hours at 90 °C in toluene. Calibrated to PS standards in THF.

monomer and crosslinker already determined, the reaction was conducted in a benchtop experiment and resulted in successful polymerisation into a uniform product, though with presence of one-armed stars or starting mRAFT agent evident in the SEC trace.

The molecular weight was somewhat attenuated from using either mRAFT agent alone, though this may be expected due to the amphiphilic nature of the crosslinked product altering the interactions in solutions. Nonetheless, production of a crosslinked polymer with uniform dispersity was achieved and to our knowledge is the first report of a miktoarm star synthesised in this way with PDMS and PEG arms.

Physical properties of star polymers

PDMS-based star polymers were isolated by precipitation into methanol however the multimodal distribution observed in the crude analysis remained. It should be noted that dissolution of most of the precipitated samples into THF proved difficult (even following gentle heating and 30 minutes of sonication), and analysis of these polymers in this solvent was unreliable (including SEC with Multi Angle Light Scattering; further discussion in ESI†). The polymers were analysed for their particle size using Dynamic Light Scattering (DLS) in methyl-isobutyl ketone (MIBK), due to incompatibilities with other solvent in regard to either refractive index or solubility. Comparison of the size (by intensity) of the 1k PDMS-EGDMA and 10k PDMS EGDMA shown in Fig. 8.

Data for all other examples is tabulated in the ESI (Table S6†), though no discernible trend was observed for the determined size compared to SEC molecular weight of the isolated products (Fig. S26†), in relation to starting arm M_n or crosslinker size (Fig. S27†).

Evaluation of the thermal properties of these polymers was undertaken by thermogravimetric analysis (TGA) under inert atmosphere (Fig. 9 and Fig. S29†). Across all samples, there was no distinct difference in the onset of degradation for polymers with different crosslinkers within the same mRAFT agent groups, though there was obvious delay in degradation between mRAFT agents used (Fig. S29†). Analysis of the PDMS mRAFT agents reveals an enhanced thermal stability with longer PDMS chains (Fig. 9a), which is to be expected. Changes in degradation rates below ~250 °C (Fig. 9a & b) may be attributed to the loss of RAFT end groups, and this is more

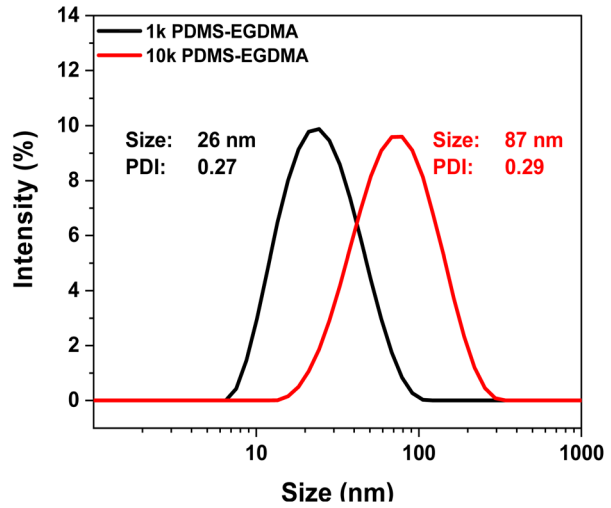

Fig. 8 Comparison of size (DLS; intensity measurement) of the 1k PDMS-EGDMA and 10k PDMS-EGDMA isolated star polymer products. Measured in MIBK.

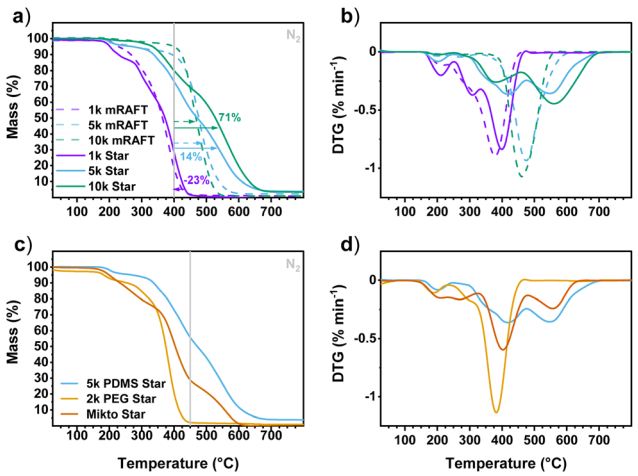

Fig. 9 (a) TGA traces of the PDMS mRAFT agents and corresponding star polymers using the EGDMA crosslinker; (b) Derivative TGA traces of the PDMS mRAFT agents and corresponding star polymers using the EGDMA crosslinker; (c) TGA traces of the 5k PDMS mRAFT, 2k PEG mRAFT and miktoarm star polymers using the EGDMA crosslinker; (d) Derivative TGA traces of the 5k PDMS mRAFT, 2k PEG mRAFT and miktoarm star polymers using the EGDMA crosslinker.

pronounced for the 1k PDMS mRAFT example given the higher relative mass fraction of the RAFT end group for this compound. Thermal stability of PDMS groups have been shown to be affected by end groups[66] and the loss of almost all residue by ~450 °C for the 1k PDMS sample may be due to some volatility of the lower M_n material.[67] Indeed, the 5k PDMS- and 10k PDMS-mRAFT agents demonstrated much greater thermal stability above 450 °C, closer to expected profiles with maximum degradation rates at ~500 °C (Fig. 9b).[66,68]

Comparing EGDMA crosslinked star polymers derived from the 1k PDMS-mRAFT agent with those from the 5k PDMS- and 10k PDMS-mRAFT agents demonstrates an elongation of the degradation profile for the latter examples (Fig. 9a). The effect of siloxane content on the thermal properties of the star polymers is exacerbated in the case of the 10k PDMS-mRAFT agent in which both the onset of degradation and the degradation profile are shifted to higher temperatures.

Interestingly, incorporation of the larger PDMS mRAFT agents into CCS structures increases the thermal stability of the whole material relative to the starting mRAFT agents (Fig. 9a). Taking the areas under the TGA curve from ≥400 °C reveals an increase of 14% and 71% for the EGDMA-based stars compared to the starting mRAFT agents (5k PDMS and 10k PDMS, respectively, Fig. 9a). This indicates that there may be some protective effect of the siloxane arms on the core, given the degradation of MMA/EGDMA copolymers has been reported to be *ca.* 400 °C.[69] This effect is not observed for the 1k PDMS mRAFT agent or star, which exhibited a 23% decrease in area above 400 °C. The reason for this is unclear, though the behaviour closely resembles that of the mRAFT agent alone. The PDMS mass fraction of these materials based on arm incorporation and monomer conversion estimates around 40% PDMS for the 1k PDMS-EGDMA star, and 70% and 81% PDMS for the 5k PDMS-EGDMA and 10k PDMS-EGDMA stars, respectively. The shift in peak degradation rate echoes this trend, with significant increase in peak degradation temperature for the longer armed stars compared to either their starting mRAFT agent or the results of the 1k PDMS compounds (Fig. 9b). Evidence of multiple degradation steps for the star materials is consistent with breakdown of the core materials (300 °C–450 °C). Incorporating other crosslinkers exhibited much the same results, though showed some slight reduction in thermal stability compared to the EGDMA versions (Fig. S29†). This effect may be due to the multimodal distribution observed by SEC for these samples which could indicate incomplete formation of a core–shell structure. Using a siloxane-based crosslinker (BMPMS) did not serve to improve thermal stability.

Analysis of the 2k PEG-EGDMA star reveals almost complete degradation of all components by *ca.* 400 °C (Fig. 9c), which is in line with the reports for both PEG and MMA/EGDMA.[69,70] The miktoarm star containing both PDMS and PEG arms is revealed to have an increased thermal stability above that of the PEG star, though still reduced compared to the PDMS version (Fig. 9c). Multiple degradation steps are observed for this sample, owing to the contributions of core, PEG and PDMS arms (Fig. 9d). Accurate assessment of the composition of these materials by TGA is still complicated, though it does provide a good indication of the protective effect from incorporating PDMS into the PEG-MMA-EGDMA structure.

Conclusions

In this work we have demonstrated the efficacy of employing the Chemspeed robot to rapidly determine compositions and optimum polymerisation conditions for generating core-crosslinked star polymers with relatively narrow molar mass disper-

sity ($Đ \approx 1.5$) and high conversion (>85%). An investigation of different crosslinkers was concurrently undertaken. It was found that the use of crosslinkers with larger distances between the methacrylate handles (DiEGDMA and above) showed an increased propensity for multimodal distribution and a reduced overall molecular weight, despite similarly high conversions of monomer components. This was ascribed to an increased incidence of intra-star as opposed to inter-star reaction of the pendent double bonds. The smallest crosslinker (EGDMA) provided the highest molar mass polymer, regardless of initial mRAFT agent molar mass. Similar findings were obtained when incorporating a mRAFT agent of different chemical structure (2k PEG mRAFT agent). Future investigation of producing stars with lower core crosslink density may benefit from larger crosslinkers with limited chain flexibility.

Most star polymers demonstrated consistent sizes (~20–40 nm) by DLS (using intensity) regardless of initial arm length, crosslinker size or final molecular weight. Thermogravimetric analysis revealed a delayed onset and elongated degradation profile for samples with increased siloxane content contributed by the starting arms. No obvious dependence of thermal stability on crosslinker type was evident. Incorporating the PDMS mRAFT agents into CCS polymers resulted in improved thermal stability over the PDMS mRAFT agent alone, or stars made from PEG arms.

This work reports the synthesis of crosslinked, siloxane-containing polymers with improved thermal stability compared to either PEG- or mikto-arm star variants. These materials have potential relevance to coating and biomedical applications.

Author contributions

D. J. E.: Conceptualisation, data curation, formal analysis, investigation, methodology, validation, visualisation, writing – original draft, writing – review & editing; S. H.: Data curation, investigation, methodology; G. M.: Funding acquisition, formal analysis, methodology, supervision, validation, writing – review & editing; B. W. M.: Funding acquisition, data curation, investigation, methodology, supervision, validation, writing – review & editing; A. P.: Formal analysis, methodology, supervision, validation, writing – review & editing; R. S.: Funding acquisition, methodology, supervision, validation, writing – review & editing.

Conflicts of interest

There are no conflicts to declare.

Acknowledgements

D. J. E. would like to acknowledge CSIRO for a Research + Postdoctoral Fellowship. Thanks to M. Hickey, L. Famularo and Y. Gozukara (CSIRO, Manufacturing) for assistance with SEC and TGA. Thanks to R. Mulder and J. Cosgriff for assistance with NMR spectroscopy. Thanks to Z. Mossayebi and G. Qiao (University of Melbourne) for assistance with SEC-MALS.

References

1 H. E. H. Meijer and L. E. Govaert, *Prog. Polym. Sci.*, 2005, **30**, 915–938.
2 H. Gao and K. Matyjaszewski, *Prog. Polym. Sci.*, 2009, **34**, 317–350.
3 H. Gao, *Macromol. Rapid Commun.*, 2012, **33**, 722–734.
4 J. M. Ren, T. G. McKenzie, Q. Fu, E. H. H. Wong, J. Xu, Z. An, S. Shanmugam, T. P. Davis, C. Boyer and G. G. Qiao, *Chem. Rev.*, 2016, **116**, 6743–6836.
5 W. Wu, W. Wang and J. Li, *Prog. Polym. Sci.*, 2015, **46**, 55–85.
6 Y. Gao, D. Zhou, J. Lyu, A. Sigen, Q. Xu, B. Newland, K. Matyjaszewski, H. Tai and W. Wang, *Nat. Rev. Chem.*, 2020, **4**, 194–212.
7 N. Hadjichristidis, M. Pitsikalis, H. Iatrou, P. Driva, G. Sakellariou and M. Chatzichristidi, in *Polymer Science: A Comprehensive Reference*, ed. K. Matyjaszewski, and M. Möller, 2012, pp. 29–111.
8 N. Hadjichristidis, M. Pitsikalis, P. G. Fragouli, I. Choinopoulos, D. Stavroulaki, V. Athanasiou and H. Iatrou, *Macromolecular Engineering*, 2022, pp. 1–76.
9 A. D. Jenkins, R. G. Jones and G. Moad, *Pure Appl. Chem.*, 2009, **82**, 483–491.
10 N. Corrigan, K. Jung, G. Moad, C. J. Hawker, K. Matyjaszewski and C. Boyer, *Prog. Polym. Sci.*, 2020, **111**, 101311.
11 A. J. Pasquale and T. E. Long, *J. Polym. Sci., Part A: Polym. Chem.*, 2001, **39**, 216–223.
12 Y. Miura and H. Dote, *J. Polym. Sci., Part A: Polym. Chem.*, 2005, **43**, 3689–3700.
13 M. Lee and H. W. Gibson, *Macromolecules*, 2020, **53**, 5399–5407.
14 B.-S. Kim, H. Gao, A. A. Argun, K. Matyjaszewski and P. T. Hammond, *Macromolecules*, 2009, **42**, 368–375.
15 Y. Pan, Y. Xue, J. Snow and H. Xiao, *Macromol. Chem. Phys.*, 2015, **216**, 511–518.
16 M. Stenzel-Rosenbaum, T. P. Davis, V. Chen and A. G. Fane, *J. Polym. Sci., Part A: Polym. Chem.*, 2001, **39**, 2777–2783.
17 J. Hu, R. Qiao, M. R. Whittaker, J. F. Quinn and T. P. Davis, *Aust. J. Chem.*, 2017, **70**, 1161.
18 M. H. Stenzel and T. P. Davis, *J. Polym. Sci., Part A: Polym. Chem.*, 2002, **40**, 4498–4512.
19 G. Moad, *Polym. Int.*, 2015, **64**, 15–24.
20 S. Allison-Logan, F. Karimi, M. D. Nothling and G. G. Qiao, *RAFT Polymerisation*, 2021, pp. 983–1015.
21 T. G. Floyd, S. Häkkinen, M. Hartlieb, A. Kerr and S. Perrier, *RAFT Polymerisation*, 2021, pp. 933–981.

22 C. Bray, R. Peltier, H. Kim, A. Mastrangelo and S. Perrier, *Polym. Chem.*, 2017, **8**, 5513–5524.
23 A. Gozgen, A. Dag, H. Durmaz, O. Sirkecioglu, G. Hizal and U. Tunca, *J. Polym. Sci., Part A: Polym. Chem.*, 2009, **47**, 497–504.
24 Y. Miura, A. Narumi, S. Matsuya, T. Satoh, Q. Duan, H. Kaga and T. Kakuchi, *J. Polym. Sci., Part A: Polym. Chem.*, 2005, **43**, 4271–4279.
25 T. He, D. Li, X. Sheng and B. Zhao, *Macromolecules*, 2004, **37**, 3128–3135.
26 C. L. Moad and G. Moad, *Chem. Teach. Int.*, 2021, **3**, 3–17.
27 G. Moad, in *Macromolecular Engineering*, ed. N. Hadjichristidis, Y. Gnanou, K. Matyjaszewski and M. Muthukumar, Wiley VCH, 2022, pp. 1–61.
28 G. Moad and E. Rizzardo, in *RAFT Polymerisation*, ed. G. Moad and E. Rizzardo, Wiley VCH, Weinheim, 2021, pp. 1–13.
29 J. Ferreira, J. Syrett, M. Whittaker, D. Haddleton, T. P. Davis and C. Boyer, *Polym. Chem.*, 2011, **2**, 1671.
30 X. Wei, G. Moad, B. W. Muir, E. Rizzardo, J. Rosselgong, W. Yang and S. H. Thang, *Macromol. Rapid Commun.*, 2014, **35**, 840–845.
31 X. Wei, P. A. Gunatillake, G. Moad, E. Rizzardo, J. Rosselgong, W. Yang and S. H. Thang, *Sci. China: Chem.*, 2014, **57**, 995–1001.
32 D. J. Wilson, D. H. Chenery, H. K. Bowring, K. Wilson, R. Turner, J. Maughan, P. J. West and C. W. G. Ansell, *J. Biomater. Sci., Polym. Ed.*, 2005, **16**, 449–472.
33 S. Sommer, A. Ekin, D. C. Webster, S. J. Stafslien, J. Daniels, L. J. Vanderwal, S. E. M. Thompson, M. E. Callow and J. A. Callow, *Biofouling*, 2010, **26**, 961–972.
34 S. Marceaux, C. Bressy, F.-X. Perrin, C. Martin and A. Margaillan, *Prog. Org. Coat.*, 2014, **77**, 1919–1928.
35 S. Wooh and D. Vollmer, *Angew. Chem., Int. Ed.*, 2016, **55**, 6822–6824.
36 P. Muthiah, B. Bhushan, K. Yun and H. Kondo, *J. Colloid Interface Sci.*, 2013, **409**, 227–236.
37 J. E. Mark, *Acc. Chem. Res.*, 2004, **37**, 946–953.
38 E. Guazzelli, E. Martinelli, L. Pelloquet, J.-F. Briand, A. Margaillan, R. Bunet, G. Galli and C. Bressy, *Biofouling*, 2020, **36**, 378–388.
39 T. H. Duong, C. Bressy and A. Margaillan, *Polymer*, 2014, **55**, 39–47.
40 N. B. Pramanik, P. Mondal, R. Mukherjee and N. K. Singha, *Polymer*, 2017, **119**, 195–205.
41 X. Qin, Y. Li, F. Zhou, L. Ren, Y. Zhao and X. Yuan, *Appl. Surf. Sci.*, 2015, **328**, 183–192.
42 Y. S. Vysochinskaya, V. V. Gorodov, A. A. Anisimov, K. L. Boldyrev, M. I. Buzin, A. V. Naumkin, K. I. Maslakov, A. S. Peregudov, O. I. Shchegolikhina and A. M. Muzafarov, *Russ. Chem. Bull.*, 2017, **66**, 1094–1098.
43 Y. S. Vysochinskaya, A. A. Anisimov, A. S. Peregudov, A. S. Dubovik, V. N. Orlov, Y. N. Malakhova, A. A. Stupnikov, M. I. Buzin, G. G. Nikiforova, V. G. Vasil'Ev, O. I. Shchegolikhina and A. M. Muzafarov, *J. Polym. Sci., Part A: Polym. Chem.*, 2019, **57**, 1233–1246.
44 P.-F. Jin, Y. Shao, G.-Z. Yin, S. Yang, J. He, P. Ni and W.-B. Zhang, *Macromolecules*, 2018, **51**, 419–427.
45 T. Ogawa, T. Suzuki and I. Mita, *Macromol. Chem. Phys.*, 1994, **195**, 1973–1983.
46 A. W. Bosman, A. Heumann, G. Klaerner, D. Benoit, J. M. J. Fréchet and C. J. Hawker, *J. Am. Chem. Soc.*, 2001, **123**, 6461–6462.
47 S. Cosson, M. Danial, J. R. Saint-Amans and J. J. Cooper-White, *Macromol. Rapid Commun.*, 2017, **38**, 1600780.
48 C. Chen, F. Richter, J. Zhang, C. Guerrero-Sanchez, A. Traeger, U. S. Schubert, A. Feng and S. H. Thang, *Eur. Polym. J.*, 2021, **160**, 110777.
49 A. J. Gormley, J. Yeow, G. Ng, Ó. Conway, C. Boyer and R. Chapman, *Angew. Chem., Int. Ed.*, 2018, **57**, 1557–1562.
50 J. Yeow, R. Chapman, J. Xu and C. Boyer, *Polym. Chem.*, 2017, **8**, 5012–5022.
51 S. Oliver, L. Zhao, A. J. Gormley, R. Chapman and C. Boyer, *Macromolecules*, 2019, **52**, 3–23.
52 A. Blencowe, J. F. Tan, T. K. Goh and G. G. Qiao, *Polymer*, 2009, **50**, 5–32.
53 B. Pichon, *Abstr. Pap. Am. Chem. Soc.*, 2003, **226**, U788.
54 D. Marshall, L. Sousa, V. Balan and B. Dale, Application of Chemspeed AUTOPLANT® to ammonia fiber expansion (AFEX) pretreatment using nitrogen overpressure and aqueous ammonia mixtures, The 32nd Symposium on Biotechnology for Fuels and Chemicals, 2010.
55 D. J. Marshall, V. Balan, S. Leonardo and D. E. Bruce, Application of Chemspeed AUTOPLANT (R) to Ammonia Fiber EXpansion (AFEX) pretreatment, The 31st Symposium on Biotechnology for Fuels and Chemicals, 2009.
56 A. McNally, C. K. Prier and D. W. MacMillan, *Science*, 2011, **334**, 1114–1117.
57 R. Hoogenboom, M. W. M. Fijten, C. Brändli, J. Schroer and U. S. Schubert, *Macromol. Rapid Commun.*, 2003, **24**, 98–103.
58 M. A. R. Meier, R. Hoogenboom, M. W. M. Fijten, M. Schneider and U. S. Schubert, *J. Comb. Chem.*, 2003, **5**, 369–374.
59 R. Hoogenboom, M. W. M. Fijten, M. A. R. Meier and U. S. Schubert, *Macromol. Rapid Commun.*, 2003, **24**, 92–97.
60 C. Guerrero-Sanchez, R. Yañez-Macias, M. Rosales-Guzmán, M. A. De Jesus-Tellez, C. Piñon-Balderrama, J. J. Haven, G. Moad, T. Junkers and U. S. Schubert, in *RAFT Polymerisation*, ed. G. Moad and E. Rizzardo, Wiley-VCH, Weinheim, 2021, pp. 1051–1076.
61 A. K. Tripathi, J. G. Tsavalas and D. C. Sundberg, *Macromolecules*, 2015, **48**, 184–197.
62 J. Rosselgong, S. P. Armes, W. R. S. Barton and D. Price, *Macromolecules*, 2010, **43**, 2145–2156.
63 J. Rosselgong and S. P. Armes, *Polym. Chem.*, 2015, **6**, 1143–1149.
64 J. Rosselgong and S. P. Armes, *Macromolecules*, 2012, **45**, 2731–2737.
65 J. Rosselgong, S. P. Armes, W. Barton and D. Price, *Macromolecules*, 2009, **42**, 5919–5924.

66 J. D. Jovanovic, M. N. Govedarica, P. R. Dvornic and I. G. Popovic, *Polym. Degrad. Stab.*, 1998, **61**, 87–93.
67 G. Camino, S. M. Lomakin and M. Lazzari, *Polymer*, 2001, **42**, 2395–2402.
68 A. RuaIgaj, M. Krajnc and U. Sebenik, *Polym. Sci.*, 2017, **03**.
69 K. Wnuczek, A. Puszka, Ł. Klapiszewski and B. Podkościelna, *Polymers*, 2021, **13**, 878.
70 R. Li, Y. Wu, Z. Bai, J. Guo and X. Chen, *RSC Adv.*, 2020, **10**, 42120–42127.